

Breaking the Stokes–anti-Stokes symmetry in Raman heterodyne detection of magnetic-resonance transitions

Rudolf Neuhaus, Matthew J. Sellars,* Stephen J. Bingham, and Dieter Suter
Universität Dortmund, Fachbereich Physik, 44221 Dortmund, Germany

(Received 10 July 1998)

Coherent Raman scattering can generate Stokes and anti-Stokes fields of comparable intensities. When the Raman shift is due to a magnetic resonance transition (usually in the MHz to GHz range), the Raman fields are generally detected by optical heterodyne detection, using the excitation laser as the local oscillator. In this case, the two sidebands generate beat signals at the same frequency and are therefore indistinguishable. Separation of the two contributions becomes possible, however, by superheterodyne detection with a frequency-shifted optical local oscillator. We compare the two scattering processes, and show how the symmetry between them can be broken in $\text{Pr}^{3+}:\text{YAlO}_3$. [S1050-2947(98)08412-1]

PACS number(s): 42.65.-k, 76.60.-k, 76.30.Kg, 76.70.Hb

I. INTRODUCTION

Coherent Raman scattering [1] occurs when a laser beam interacts with a resonant medium that contains a coherent excitation. Figure 1 schematically shows the simplest quantum-mechanical system that can show this effect: a coherent excitation of transition $|1\rangle \leftrightarrow |2\rangle$ is present, involving a vibrational transition [1] or a coherent superposition of different spin states [2]. Levels $|1\rangle$ and $|2\rangle$, which in this example are electronic ground states, are connected to the same excited state $|3\rangle$ through optical transitions. If the laser field couples to transition $|1\rangle \leftrightarrow |3\rangle$, it excites an optical polarization in transition $|2\rangle \leftrightarrow |3\rangle$, which is the source of the Raman field. The Raman wave is phase locked to the exciting laser field and to the excitation in the medium. Its frequency is therefore equal to the sum or difference of the frequencies of the laser field and the excitation in the medium. The scattering cross section is independent of the excitation intensity, i.e., the scattered field is directly proportional to the incident field [1].

The fixed phase relation between the Raman and driving laser fields allows one to detect the Raman field through an optical heterodyne process by letting the Raman field interfere with the excitation field on a quadratic photodetector. The resulting beat signal is proportional to the Raman field and therefore to the coherent excitation. Such an experiment, which combines radio-frequency or microwave excitation of the sample with optical heterodyne detection, is commonly referred to as the Raman heterodyne experiment [3].

One important application of coherent Raman scattering is the detection of nuclear [3] and electronic [4–6] spin transitions. In all such systems studied to date, the width of the optical transitions is large compared to the frequency of the spin transition. The laser can couple to either of the two optical transitions. The Raman field, which always appears in the third transition, may therefore have a lower frequency

(Stokes shifted) or a higher frequency (anti-Stokes shifted). The transmitted light then contains both sidebands with comparable intensity. In the Raman heterodyne experiment, the signal stems from a beat between the unscattered laser beam and the Stokes or anti-Stokes scattered light. Both Raman fields generate signals at the same frequency and the observed signal contains contributions from both scattering processes.

If the two Raman sidebands are equal in amplitude and phase, the optical field (consisting of the laser field and the two sidebands) shows a pure amplitude modulation, which is measured by the photodetector. If the two scattering processes that give rise to the two sidebands are not completely symmetric, i.e., if the two sidebands have different amplitudes, the optical field is also frequency modulated. However, since the detector is not sensitive to frequency modulation, this asymmetry is normally not detected. A measurement of an imbalance of the Raman sidebands would therefore require the conversion of the optical frequency modulation (fm) into amplitude modulation (am). This is possible, for example, by shifting the phase of the laser field with respect to the sidebands. In a typical Raman heterodyne experiment, this can only be achieved if the polarization of the carrier differs from that of the sidebands: in such a sys-

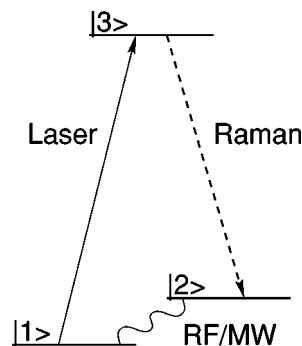


FIG. 1. Principle of coherent Raman scattering. Transition $|1\rangle \leftrightarrow |2\rangle$ is excited by a resonant rf/mw field. The laser field couples the ground state $|1\rangle$ to the excited state $|3\rangle$, and creates a coherence in both optical transitions, including $|2\rangle \leftrightarrow |3\rangle$, which is the source of the Raman field.

*Present address: Laser Physics Center, Research School of Physical Sciences and Engineering, Australian National University, Canberra, ACT 0200, Australia.

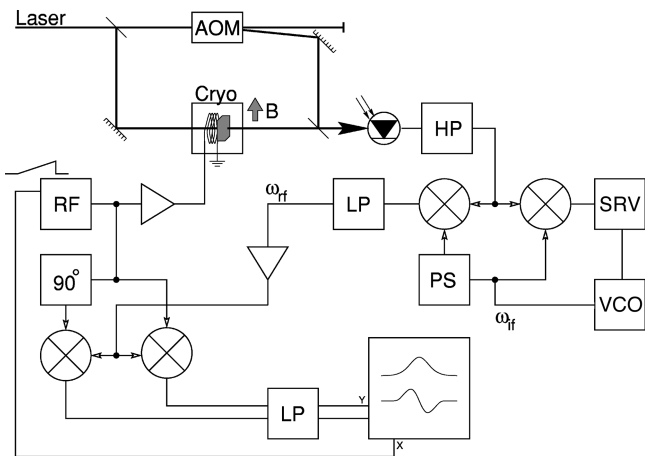


FIG. 2. Experimental setup: AOM is the acousto-optic modulator, HP is the high-pass filter, SRV is the servoloop, VCO is the voltage controlled oscillator, PS is the phase shifter, LP are low-pass filters, RF is the RF sweep generator, and 90° is a $\pi/2$ phase delay.

tem, a birefringent optical element can implement the phase shift, as has been demonstrated experimentally by Mlynek *et al.* [6] on a transition in an atomic vapor.

In solid materials, the Raman fields are usually not orthogonal to the exciting field. In this paper, we present a technique which allows the separation of Stokes and anti-Stokes contributions for arbitrary polarizations of the sidebands. For this purpose, we use optical superheterodyne detection of the Raman fields with a local oscillator that is frequency shifted with respect to the excitation laser. The Stokes and anti-Stokes components are thereby converted into rf signals with different frequencies. A second demodulation of these signals, using conventional radio-frequency electronics, yields the am and fm amplitudes of the optical signal, which can be recombined into the amplitudes of Stokes and anti-Stokes fields.

As noted above, coherent Raman scattering should yield similar amplitudes of Stokes and anti-Stokes components. This has been confirmed experimentally in one case [6]. However, in inhomogeneously broadened systems, the two scattering processes are due to different groups of atomic ions or molecules. Here it is possible to manipulate the two groups such that the cross sections for the two scattering processes differ, resulting in different amplitudes for the two sidebands. We have experimentally verified this possibility for a crystal of $\text{Pr}^{3+}:\text{YAlO}_3$.

II. THEORY

We consider the three-level system of Fig. 1. The coherent excitation of the medium is generated by a microwave (mw) or radio frequency (rf) field that couples to the transition $|1\rangle \leftrightarrow |2\rangle$. If the populations ρ_{11} and ρ_{22} of the two levels are different, the rf or mw field excites a coherence ρ_{12} in this transition, which in the absence of saturation is proportional to the population difference, to the rf field strength B_1 , and to the magnetic dipole matrix element μ_{12} for this transition [3],

$$\rho_{12} = \alpha(\rho_{22} - \rho_{11})B_1\mu_{12}.$$

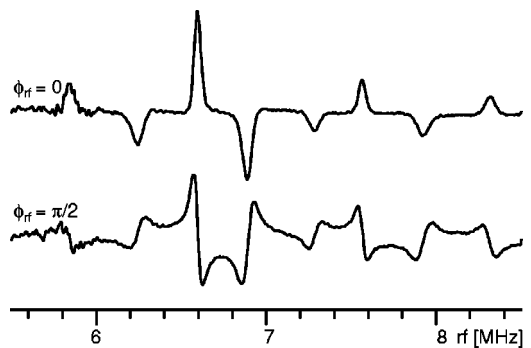


FIG. 3. am components ($\phi_{if}=0$) of the Raman heterodyne spectrum for the ground-state $|\pm \frac{1}{2}\rangle \leftrightarrow |\pm \frac{3}{2}\rangle$ transitions of $\text{Pr}^{3+}:\text{YAlO}_3$.

A test laser field $E_1 = E_L e^{i(\omega_L t + \phi_L)}$, resonant with the transition $|1\rangle \leftrightarrow |3\rangle$ with matrix element μ_{13} , couples this coherence to a different electronic state $|3\rangle$. Through this resonant interaction the initial superposition state between sublevels $|1\rangle$ and $|2\rangle$ is transformed into a new superposition state which also contains coherence in the optical transition between the electronically excited state $|3\rangle$ and the ground-state sublevel $|2\rangle$

$$\rho_{23} = \beta(\rho_{22} - \rho_{11})B_1\mu_{12}E_1\mu_{13}.$$

This optical coherence is therefore proportional to the coherence in the magnetic transition and to the optical Rabi frequency $E_L\mu_{13}$.

Macroscopically, this optical coherence corresponds to a polarization

$$P_{23} = \beta(\rho_{22} - \rho_{11})B_1E_1\mu_{12}\mu_{13}\mu_{23}. \quad (1)$$

This polarization is the source of the Raman field, and is therefore proportional to the population difference between the two ground-state sublevels, and to the product of the three matrix elements for the three transitions in this system. This is a significant difference from the usually observed proportionality to the square of a single matrix element, and is the basis for various interference effects [7–10], such as the one between Stokes and anti-Stokes field discussed here.

The Stokes and anti-Stokes fields can be written in the usual complex notation as

$$E_S = E_- e^{i(\omega_L - \omega_{if})t},$$

$$E_{AS} = E_+ e^{i(\omega_L + \omega_{if})t},$$

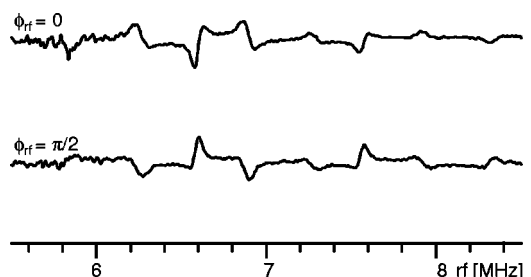


FIG. 4. fm components ($\phi_{if}=\pi/2$) of the Raman heterodyne spectrum for the ground-state $|\pm \frac{1}{2}\rangle \leftrightarrow |\pm \frac{3}{2}\rangle$ transitions of $\text{Pr}^{3+}:\text{YAlO}_3$.

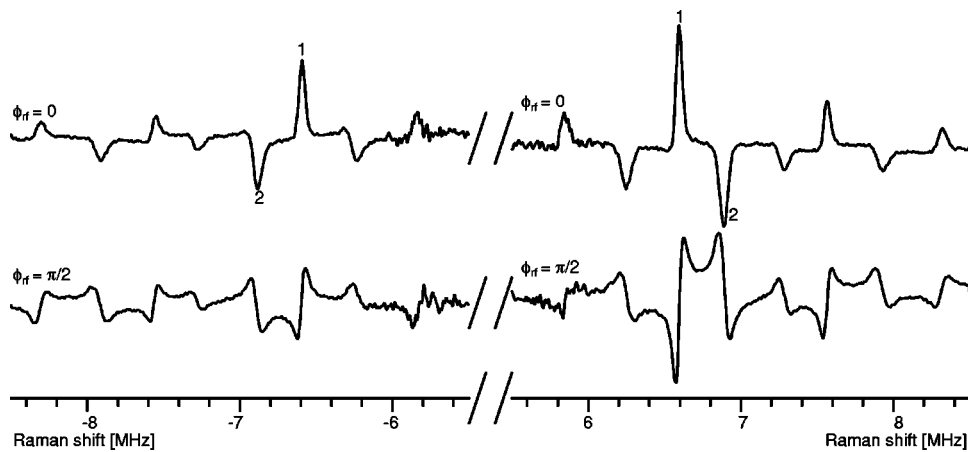


FIG. 5. Stokes (left) and anti-Stokes (right) components of the signal.

where

$$E_{\pm} = (a_{\pm} + ib_{\pm})$$

are the slowly varying amplitudes of the sidebands. The beat signal at ω_{rf} with the local oscillator E_1 has two components

$$E_S E_1^* + c.c. = (a_- + ib_-) E_L^* e^{i(-\omega_{rf}t - \varphi_L)} + c.c., \quad (2)$$

$$E_{AS} E_1^* + c.c. = (a_+ + ib_+) E_L^* e^{i(\omega_{rf}t - \varphi_L)} + c.c. \quad (3)$$

The combined signal is proportional to the sum of Eqs. (2) and (3):

$$\begin{aligned} \text{Re}\{(E_S + E_{AS})E_1^*\} &\propto a_- \cos(\omega_{rf}t + \varphi_L) + b_- \sin(\omega_{rf}t + \varphi_L) \\ &+ a_+ \cos(\omega_{rf}t - \varphi_L) - b_+ \sin(\omega_{rf}t - \varphi_L). \end{aligned} \quad (4)$$

In a normal Raman heterodyne experiment, where the exciting laser is the local oscillator, the phase φ_L of the local oscillator is fixed to $\varphi_L = 0$, and the signal is proportional to

$$S_{rf}^{\varphi_L=0} = (a_- + a_+) \cos(\omega_{rf}t) + (b_- - b_+) \sin(\omega_{rf}t). \quad (5)$$

The real parts of the amplitudes add, while the imaginary parts subtract. The two components can be measured separately by phase-sensitive detection, using the radio frequency as a reference. Thus the standard detection scheme measures the am component of the signal, to which the two sidebands contribute equally and in phase.

If the phase of the local oscillator can be shifted by $\pi/2$ the signal is proportional to

$$S_{rf}^{\varphi_L=\pi/2} = (b_- + b_+) \cos(\omega_{rf}t) + (a_+ - a_-) \sin(\omega_{rf}t). \quad (6)$$

This component may be considered as the fm component of the signal.

If it is possible to shift the phase of the carrier, four independent measurements can be made (two for each rf phase), and a straightforward linear combination of these data yields the complex amplitudes of the two optical sidebands. If the polarization of the sidebands is orthogonal to the carrier, a phase shift can be introduced by placing a retardation plate in front of the detector [6].

If the polarization of the sidebands is not orthogonal to the carrier, which is the case in most solids, this technique is not applicable, and a local oscillator that can be manipulated independently of the excitation laser beam must be used. When an independent local oscillator is superimposed over the transmitted laser beam, two problems may arise: (i) the beat signals involving the independent local oscillator might not be separated from those of the transmitted laser beam, and (ii) vibrations and other instabilities that act differently on the two laser beams introduce phase noise.

These technical problems can be avoided by using an independent local oscillator that is frequency shifted with respect to the exciting laser by ω_{if} . With this shift, the beat signals between the two Raman sidebands and the local oscillator appear at $\omega_{if} \pm \omega_{rf}$. Simultaneously, the beat signal between the transmitted laser beam and the frequency-shifted

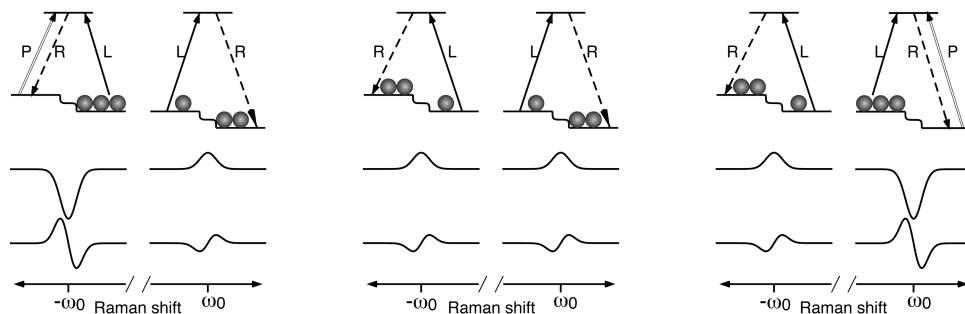


FIG. 6. Level diagrams and theoretical spectra for the Stokes and anti-Stokes components of a single magnetic resonance transition. The left pair shows a situation with a pump beam with $\omega_p - \omega_L = -\omega_0$, the middle without a pump beam, and the right for $\omega_p - \omega_L = \omega_0$.

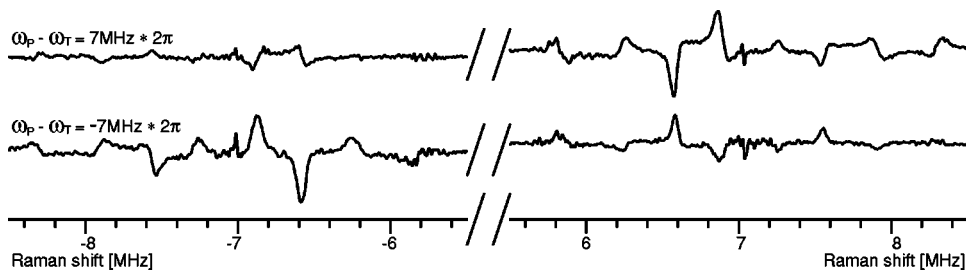


FIG. 7. Stokes (left) and anti-Stokes (right) components of the signal with a pump beam shifted by $+7$ MHz (upper trace) and -7 MHz (lower trace).

local oscillator appears as a strong radio-frequency signal at ω_{if} . The optical signal is thus converted down to the radio-frequency range, where standard techniques are available for phase-sensitive detection. Using the signal at ω_{if} with a variable phase shift as an rf local oscillator, a second demodulation stage converts the signal to the original Raman beat frequency ω_{rf} . This two-stage demodulation scheme, which corresponds to a superheterodyne experiment, allows one to measure the four signals of Eqs. (5) and (6) independently.

III. RAMAN SUPERHETERODYNE DETECTION

To verify these predictions, we performed experiments on the $^3\text{H}_4 \leftrightarrow ^1\text{D}_2$ transition of Pr^{3+} in the crystal $\text{Pr}^{3+}:\text{YAlO}_3$ at 610.7 nm, as in a number of earlier Raman heterodyne experiments [7,9,11]. The Pr^{3+} concentration was 0.1 at. %, and the sample was cooled to approximately 4 K in a He flow cryostat. Figure 2 shows the experimental setup. The laser beam was derived from a tunable ring dye laser (Coherent 899-21) and focused to a spot size diameter of 0.6 mm with a power of ≈ 2.3 mW and applied along the c axis of the crystal. The rf magnetic field, also applied along the c axis, had an amplitude of approx. 0.15 G. Its frequency was swept through the ground state $|\pm \frac{1}{2}\rangle \leftrightarrow |\pm \frac{3}{2}\rangle$ hyperfine transitions around 7 MHz. A static magnetic field of 69 G was applied perpendicular to the c axis. In this geometry, all four transitions from the $|\pm \frac{1}{2}\rangle$ to the $|\pm \frac{3}{2}\rangle$ states have comparable intensities. The two crystallographically inequivalent sites can be distinguished by their opposite sign and result in an eight-line spectrum, which is clearly resolved in Fig. 3.

Part of the incident laser beam was split off in front of the sample and shifted in frequency with an acousto-optic modulator by $\omega_{\text{if}}=80$ MHz. This beam was used as the second local oscillator by recombining it with the beam transmitted

through the sample. The signal was detected with a home-built photodetector. A high-pass filter retains only the signal contributions around ω_{if} (resulting from the interference between the laser and the frequency-shifted local oscillator and $\omega_{\text{if}} \pm \omega_{\text{rf}}$ that represent the down-converted Raman signal).

All three signal components at this stage contain phase noise from mechanical instabilities acting on the different beam paths of signal laser beam and local oscillator beam. It can be eliminated by using the 80-MHz center band as the second local oscillator to demodulate the Raman signals. For this purpose, we phase locked a voltage-controlled oscillator (VCO) to the centerband at ω_{if} . The VCO signal, with an appropriate phase shift, was then used as a second local oscillator to demodulate the Raman signals according to Eqs. (5) and (6).

The resulting dc signal depends on the phases of the two radio-frequency local oscillators φ_{if} and φ_{rf} , which are independent variables. We obtain therefore four independent measurements from which the sideband amplitudes a_{\pm} and b_{\pm} can be calculated:

$$a_{\pm} \propto S(\varphi_{\text{if}}=0, \varphi_{\text{rf}}=0) \pm S\left(\varphi_{\text{if}}=\frac{\pi}{2}, \varphi_{\text{rf}}=\frac{\pi}{2}\right), \quad (7)$$

$$b_{\pm} \propto S\left(\varphi_{\text{if}}=\frac{\pi}{2}, \varphi_{\text{rf}}=0\right) \mp S\left(\varphi_{\text{if}}=0, \varphi_{\text{rf}}=\frac{\pi}{2}\right).$$

IV. EXPERIMENTAL RESULTS AND DISCUSSION

A. Symmetrical scattering

For all experimental results presented in this section, the rf excitation frequency was scanned from 5.5 to 8.5 MHz.

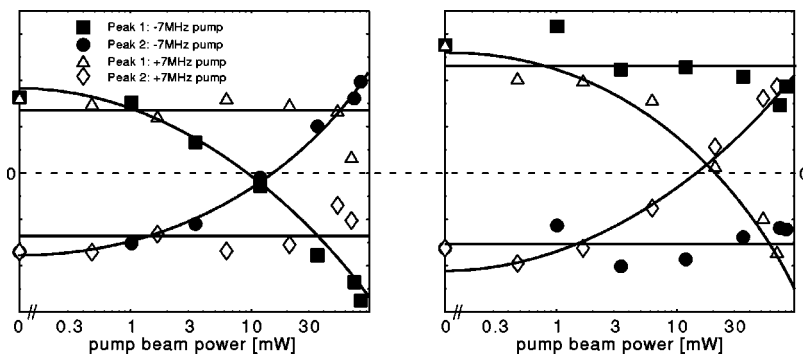


FIG. 8. Amplitudes of the Stokes (left) and anti-Stokes (right) components of two peaks (1 and 2 as marked in Fig. 5) of the spectrum with a pump beam shifted by ± 7 MHz plotted against the pump beam power. The lines are only guides to the eye.

An example of a resulting Raman heterodyne spectrum is shown in Fig. 3. For this measurement, the phase of the local oscillator φ_{if} was adjusted to zero. The two traces with absorption and dispersion type line shapes correspond to two orthogonal phases of the rf local oscillator. We define the phase $\varphi_{\text{rf}}=0$ for the upper trace, corresponding to $\varphi_{\text{rf}}=\pi/2$ for the lower trace. As discussed in Sec. II, this is the conventional Raman heterodyne signal, resulting from the amplitude modulation of the laser field, to which Stokes and anti-Stokes sidebands contribute equally.

Figure 4 contains the same data with the 80-MHz local oscillator shifted in phase by $\pi/2$. The rf phases are the same as in Fig. 3. As expected from theoretical considerations [3] and earlier measurements [6], this signal is significantly smaller, indicating that Stokes and anti-Stokes sidebands have comparable amplitudes.

Linear combination of these data according to Eqs. (7) converts them into the amplitudes of Stokes and anti-Stokes sidebands. The resulting spectra are shown in Fig. 5. The left-hand side shows the Stokes component (negative Raman shift), while the anti-Stokes component is shown on the right.

In the system considered here, the symmetry between Stokes and anti-Stokes scattering apparent in these spectra arises from the macroscopic average over the inhomogeneously broadened ensemble of ions. An individual ion contributes either to the Stokes or anti-Stokes sideband, as represented schematically in the center part of Fig. 6, which summarizes the standard Raman heterodyne experiment. If the homogeneous optical linewidth and the laser frequency jitter are both small compared to the Raman shift, the population difference between the two spin levels is generated by spectral holeburning due to the laser beam. Depending on the spectral shift of the individual ion, the laser can be resonant with either of the two optical transitions. For the two types of ions contributing to the signal, the population difference is roughly reversed, resulting in equal amplitudes for the Raman sidebands generated by these subsets of ions. This is indicated in the lower half of Fig. 6, where the resulting rf signals due to the two groups of ions are represented.

B. Asymmetrical scattering

The above picture suggests a possible way for modifying the Stokes–anti-Stokes symmetry: if the population difference in one of the two groups of ions is modified, e.g., by an additional pump laser beam [12], this should affect only one of the two sidebands. Two possible situations are represented in Fig. 6: On the left, an additional pump laser beam, whose frequency has been shifted by the ground state splitting $-\omega_0$ with respect to the test laser, interacts with the ions that contribute to the Stokes sideband, while it is not resonant with the other group of ions. The modification of the population difference results in an inverted Raman signal for the Stokes component. The opposite case, where the pump laser is shifted to higher frequencies, is represented on the right-hand side of the figure; here we expect an inversion of the anti-Stokes component.

For the experimental implementation we used acousto-optic modulators to frequency shift the pump laser with respect to the test laser. Aside from the additional pump laser

beam, the experiment and the data analysis were identical to the case without the pump laser beam discussed above. Examples of resulting spectra are shown in Fig. 7; the upper trace corresponds to the up-shifted pump laser. We clearly see that the amplitude of the anti-Stokes line is inverted with respect to the reference spectrum represented in Fig. 5, while the sign of the Stokes component is the same. A pump laser shifted to lower frequencies inverts the sign of the Stokes component, as shown in the lower trace.

Figure 8 displays the measured integrals over the two peaks, marked in Fig. 5 as 1 and 2. The amplitudes of the peaks are shown for the Stokes (left) and anti-Stokes (right) components of the signal as a function of the pump power for frequency shifts of the pump beam of ± 7 MHz. The Stokes components with a negative shift of the pump frequency and the anti-Stokes components for a positive shift gradually change sign going through zero, while the other components stay roughly constant.

The two figures clearly demonstrate that a pump laser beam which modifies the populations of specific subsets of ions in an inhomogeneously broadened system can break the symmetry between Stokes and anti-Stokes sidebands in coherent Raman scattering. The amplitudes of the opposite group of ions, which should not be affected, are smaller than in the absence of the pump laser beam. While this effect is not completely understood, it is probably due to heating by the pump laser.

V. CONCLUSION

In most systems, where magnetic resonance transitions have been investigated by Raman heterodyne detection, the width of the optical transitions is large compared to the frequency of the spin transition. For such systems it is well known that Stokes and anti-Stokes scattering are equivalent to a large degree. Numerous Raman-heterodyne experiments have measured amplitude-modulated optical signals, which arise from the superimposed contributions of the upper and lower sidebands. In one case [6], where the polarization of the signal was orthogonal to the carrier, it was verified that the fm contribution to the signal is small compared to the am part.

In this paper, we have presented an experimental technique that permits measurements of both sidebands for arbitrary polarizations. Application of this technique to an inhomogeneously broadened ionic crystal shows that the symmetry between the two sidebands is also present in this case. It can be broken, however, if one of the sets of ions contributing to the signal is selectively modified. In the example presented here, we chose a pump laser beam that inverts the population difference between the two sublevels. The symmetry between the two sidebands, which is broken here, should be better conserved in homogeneously broadened systems, where all centers contribute to both sidebands.

ACKNOWLEDGMENTS

This work was supported by DFG Grant No. Su 192/4-1. M.S. acknowledges support by the DFG through the Graduiertenkolleg Festkörperspektroskopie, and S.J.B. was supported by the Royal Society, London.

- [1] J. A. Giordmaine and W. Kaiser, *Phys. Rev.* **144**, 676 (1966).
- [2] R. G. Brewer and E. L. Hahn, *Phys. Rev. A* **8**, 464 (1973).
- [3] N. C. Wong *et al.*, *Phys. Rev. B* **28**, 4993 (1983).
- [4] K. Holliday, X.-F. He, P. T. H. Fisk, and N. B. Manson, *Opt. Lett.* **15**, 983 (1990).
- [5] S. J. Bingham, D. Suter, A. Schweiger, and A. J. Thomson, *Chem. Phys. Lett.* **266**, 543 (1997).
- [6] J. Mlynek, C. Tamm, E. Buhr, and N. C. Wong, *Phys. Rev. Lett.* **53**, 1814 (1984).
- [7] M. Mitsunaga, E. S. Kintzer, and R. G. Brewer, *Phys. Rev. Lett.* **52**, 1484 (1984).
- [8] D. R. Taylor, *Opt. Commun.* **52**, 204 (1984).
- [9] M. Mitsunaga, E. S. Kintzer, and R. G. Brewer, *Phys. Rev. B* **31**, 6947 (1985).
- [10] T. Blasberg and D. Suter, *Phys. Rev. B* **51**, 12 439 (1995).
- [11] L. E. Erickson, *Phys. Rev. B* **42**, 3789 (1990).
- [12] T. Blasberg and D. Suter, *Phys. Rev. B* **48**, 9524 (1993).